

# MEDUHIP: TOWARDS HUMAN-IN-THE-LOOP MEDICAL SEGMENTATION

**Jiayuan Zhu**  
University of Oxford  
jiayuan.zhu@ieee.org

**Junde Wu \***  
University of Oxford  
jundewu@ieee.org

## ABSTRACT

Although segmenting natural images has shown impressive performance, these techniques cannot be directly applied to medical image segmentation. Medical image segmentation is particularly complicated by inherent uncertainties. For instance, the ambiguous boundaries of tissues can lead to diverse but plausible annotations from different clinicians. These uncertainties cause significant discrepancies in clinical interpretations and impact subsequent medical interventions. Therefore, achieving quantitative segmentations from uncertain medical images becomes crucial in clinical practice. To address this, we propose a novel approach that integrates an **uncertainty-aware model** with **human-in-the-loop interaction**. The uncertainty-aware model proposes several plausible segmentations to address the uncertainties inherent in medical images, while the human-in-the-loop interaction iteratively modifies the segmentation under clinician supervision. This collaborative model ensures that segmentation is not solely dependent on automated techniques but is also refined through clinician expertise. As a result, our approach represents a significant advancement in the field which enhances the safety of medical image segmentation. It not only offers a comprehensive solution to produce quantitative segmentation from inherent uncertain medical images, but also establishes a synergistic balance between algorithmic precision and clinician knowledge. We evaluated our method on various publicly available multi-clinician annotated datasets: REFUGE2, LIDC-IDRI and QUBIQ. Our method showcases superior segmentation capabilities, outperforming a wide range of deterministic and uncertainty-aware models. We also demonstrated that our model produced significantly better results with fewer interactions compared to previous interactive models. We will release the code to foster further research in this area.

## 1 INTRODUCTION

Medical image segmentation plays an indispensable role in disease diagnosis, prognosis monitoring and anatomy delineation Mei et al. (2020); Wang et al. (2019b); Zhu et al. (2019). With the rapid development of artificial intelligence in recent decades, an enormous number of deep learning models have been applied in clinics to assist medical image segmentation Litjens et al. (2017); Liu et al. (2021). These medical image segmentation models often employ techniques initially developed for natural images and then modified for medical applications. Despite the apparent success of these adaptations Chen et al. (2021); Ronneberger et al. (2015); Tajbakhsh et al. (2016), they often overlook the unique challenges inherent in medical images Hesamian et al. (2019).

Unlike natural images, which are characterised by clear and distinct patterns, medical images typically exhibit ambiguous boundaries due to varying tissue contrast and overlapping anatomical structures Hesamian et al. (2019). Even different professional clinicians may provide different annotations for the same medical image, reflecting a unique level of uncertainty not seen in natural images. This uncertainty causes incomplete version of the ground truth, potentially resulting in unpredictable clinical outcomes Cabitza et al. (2018); Garcia et al. (2015). Therefore, developing methodologies specifically to manage the uncertainties inherent in medical images becomes crucial.

---

\*Project Lead

A common approach to express the medical image uncertainty is generating multiple segmentations, Baumgartner et al. (2019); Kohl et al. (2019b); Lakshminarayanan et al. (2017); Rupprecht et al. (2017), mimicing the behaviour of a group of clinicians. However, this method has a major drawback, restricting direct real-world applications. Clinicians need to review and interpret numerous predicted segmentations, which can be overwhelming and time-consuming. Besides, deciding which segmentation best captures their thought can also be challenging. In the worst-case scenario, none of the generated segmentations meet the clinician’s expectations, thereby negating the potential benefits of this approach.

A human-in-the-loop interactive model can mitigate the limitations of generating multiple segmentations by incorporating clinician feedback into the segmentation process Marinov et al. (2024). This human-in-the-loop approach allows clinicians to provide real-time corrections, so they no longer need to review and interpret numerous segmentations. Instead, the model progressively improves based on clinicians’ input and moves towards clinicians’ annotation, ensuring the final segmentation satisfies the clinician. Therefore, the human-in-the-loop approach enhances efficiency and robustness, making the segmentation process more practical for real-world applications Wang et al. (2018).

In this paper, we introduce **MedUHIP**, a new paradigm that leverages both **Uncertainty-aware models** and **Human-In-the-loop** interactions. MedUHIP addresses medical image uncertainty by generating multiple segmentations and fusing them into a single soft prediction. Clinicians can modify this soft prediction through human-in-the-loop interactions, allowing the model to learn their individual preferences and thus further understand the uncertainty inherent in medical images. Subsequently, the model generates a new set of segmentations that better align with the clinicians’ interaction. Through this human-in-the-loop interaction process, the final prediction supported by the clinician becomes more suitable for direct clinical use.

In summary, our contributions are as follows:

- We introduced a novel approach, which allows iteratively modifying the prediction and captures the inherent uncertainty in the medical image.
- We proposed a model with Sampling Net module to learn clinician’s preference based on their interaction. The Sampling Net module results a sampling space which adapts towards clinician’s preference. Besides, multiple segmentations can be predicted by sampling from this space to reflect the uncertainty in medical images.
- We compared our MedUHIP approach with various deterministic and uncertainty-aware models. It consistently achieves significantly superior results on multi-clinician annotated datasets: REFUGE2, LIDC-IDRI and QUBIQ. Additionally, MedUHIP outperforms other interaction methods with fewer iterations.

## 2 RELATED WORK

**Medical Image Segmentation** Deep learning is crucial for medical image segmentation as it enhances accuracy and efficiency for various diagnostic and treatment processes Chan et al. (2020); Wang et al. (2021). Representative models like U-Net Ronneberger et al. (2015), TransUNet Chen et al. (2021), and SwinUNet Cao et al. (2021) have advanced performance by incorporating frontier computer vision techniques. U-Net is effective and simple, TransUNet captures long-range dependencies, and SwinUNet offers exceptional accuracy and scalability.

**Uncertainty Estimation** It is notable that varying tissue contrast or clinical expertise will lead to different annotations given the same medical image Sylolypavan et al. (2023). This uncertainty inherent in medical images cannot be reduced with more data or more complex model Kiureghian & Ditlevsen (2009). It can only be estimated by training the model to generate a range of potential predictions Huang et al. (2024); Zou et al. (2023). Model ensembling, label sampling Jensen et al. (2019), and multi-head strategies Guan et al. (2018) are typical methods to address uncertainty by combining multiple model predictions. ProbUNet Kohl et al. (2018), CM-Net Zhang et al. (2020) and MRNet Ji et al. (2021) model the the posterior distribution of model parameters or predictions explicitly to capture the uncertainty. However, all above techniques either produce a set of predictions or require the prior knowledge of the expertise level, hindering the wide and direct clinical use.

**Human-in-the-loop Interactive Models** Interactive medical image segmentation is essential for improving accuracy by integrating clinicians to refine automated segmentation results. Most of previous methods Luo et al. (2021); Sakinis et al. (2019); Wang et al. (2018; 2019a) encode clinician interactions (e.g. click, scribble, bounding box) into a distance map and integrate them into the CNN-based network. However, the choice of encoding strategies significantly impact the segmentation performance Luo et al. (2021). Some approaches like Segment Anything Model (SAM, Kirillov et al. (2023)) represents user interactions by positional encoding Tancik et al. (2020), which does not require extra distance map. It maps input interactions into Fourier features to capture complex spatial and temporal relationships. Despite its extraordinary performance in natural images, a series follow-up work Deng et al. (2023); Ma et al. (2024); Wu et al. (2023) in medical domain also show excellent results.

### 3 METHODOLOGY

#### 3.1 MOTIVATION

As aforementioned, the medical image uncertainty can be shown as the annotation disagreement between different clinicians. MRNet Ji et al. (2021) quantitatively proved that individual clinician has consistent segmentation patterns, while the expertise levels among different clinicians vary. We reasonably conjecture that the interaction behaviour among individual clinicians is also consistent, but it differs among clinicians. If so, we can adaptively learn the individual clinician’s preference through human-in-the-loop interaction and modify the segmentation accordingly.

We then conduct a preliminary experiment with optic cup segmentation on REFUGE2 dataset under SAM’s Kirillov et al. (2023) setting to demonstrate that clinician-specific interaction indeed impacts the segmentation performance. As we do not have the records about how each clinician provides the interaction, we mimic the behaviour through three strategies, reflecting clinicians with different expertise levels. If the clinicians have limited background knowledge, they are likely to click the image randomly. Assertive clinicians might click areas distinct to others and experienced clinicians tend to self-correct the error from last iteration. Fig. 1 shows that the segmentation performance truly depends on the interaction strategy or individual clinician’s preference. Therefore, this discovery motivated us to propose the MedUHIP model.

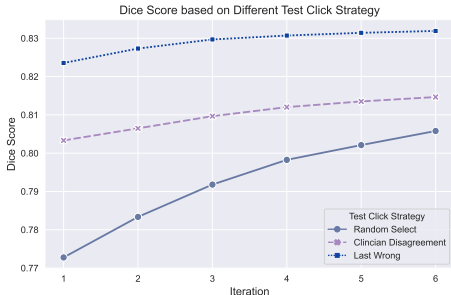


Figure 1: A preliminary experiment in testing the impact of different interaction (i.e. clicking) preferences, conducted for the optic cup segmentation on REFUGE2 test set under SAM’s structure with Dice score. It indicates that the segmentation performance significantly varies across different interaction strategies, regardless of the number of clicks.

#### 3.2 OVERALL FRAMEWORK

In this work, we propose the novel MedUHIP model to assist segmenting uncertain medical images through human-in-the-loop interaction. Fig. 2 illustrates the overall framework of our MedUHIP, which contains iterative human-model interaction steps towards the final segmentation. It ensures that the final segmentation is not only predicted by the automatic model, but also approved by the clinician, which encourages direct clinical use.

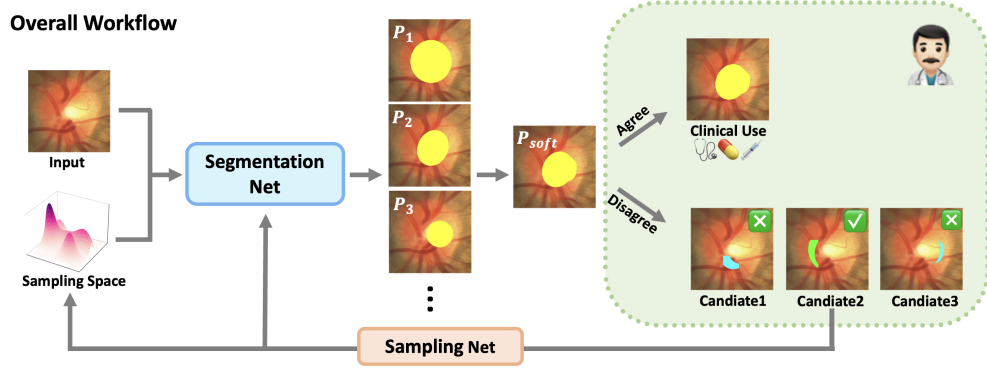


Figure 2: An overall workflow of our MedUHIP model.

In the  $t^{th}$  iteration, apart from the input image  $I$ , we also randomly draw  $N$  samples  $S_1^t, \dots, S_N^t$  from the sampling space  $SP$  to capture the image uncertainty. The combined features are sent to the Segmentation Net for automatic segmentation, generating  $N$  predictions  $P_1^t, \dots, P_N^t$ . These output segmentations are fused to produce a soft binary prediction  $P_{soft}^t$ , which can be direct used under clinician approval. If the clinician unsatisfies with  $P_{soft}^t$ , our model will offer  $K$  candidate regions  $C_1^t, \dots, C_K^t$  recommended for further improvement. These candidate regions are composed from the set of previous predicted segmentations  $P_1^t, \dots, P_N^t$ . Afterwards, the Sampling Net modifies the sampling space  $SP$  based on clinician's interaction selection, aiming to produce segmentations towards clinician's preference in the next iteration.

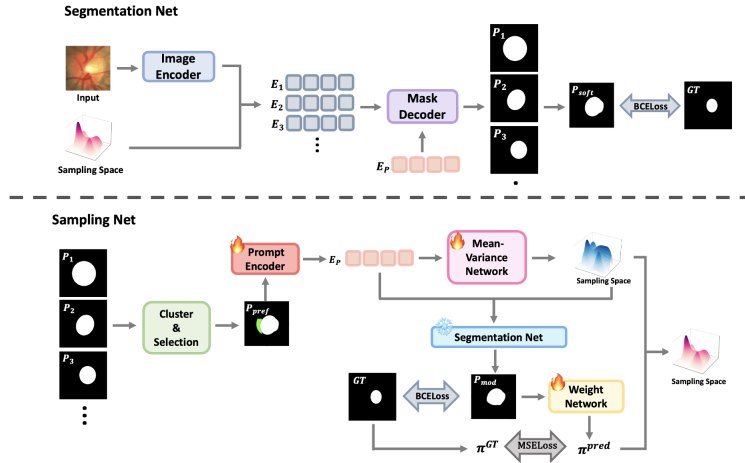


Figure 3: The architecture of Segmentation Net and Sampling Net.

### 3.3 SEGMENTATION NET

Similar to SAM Kirillov et al. (2023), our segmentation net is consisted of image encoder, prompt encoder, and mask decoder. We first obtain a general image embedding  $E_G^t$  by applying a MAE He et al. (2021) pre-trained Vision Transformer (ViT) to the input image  $I$ . Then we randomly draw  $N$  samples  $S_1^t, \dots, S_N^t$  from the sampling space  $SP$ . Each  $S_i^t$  is combined with the general image embedding  $E_G^t$  to generate a series of new image embeddings  $E_1^t, \dots, E_N^t$  by:

$$E_i^t = ReLU(Conv(E_G^t \oplus S_i^t)), i = 1, 2, \dots, N \quad (1)$$

The prompt encoder in Sampling Net maps clinician’s interaction selection to 256-dimensional vectorial embedding  $E_p^t$ . It considers both the interaction location and whether it belongs to foreground or background.

The lightweight mask decoder is a modified transformer decoder block, which integrates a dynamic mask prediction head. It utilises two-way cross-attention to enable the interaction between each image embedding  $E_i^t$  and prompt embedding  $E_p^t$ . Afterwards, it upsamples the image embedding  $E_i^t$ , and an MLP translates the output token into a dynamic linear classifier that predicts a sequence of masks  $P_1^t, \dots, P_N^t$  for the input image  $I$ . The soft prediction  $P_{soft}^t$  is calculated by majority vote from the sequence of masks, where  $\mathbb{I}(\cdot)$  is the indicator function:

$$P_{soft}^t = \mathbb{I}\left(\frac{1}{N} \sum_{i=1}^N P_i^t > \frac{1}{2}\right) \quad (2)$$

We represent all parameters in Segmentation Net as  $\theta_{Seg}$ , and update them through the cross-entropy loss function  $\mathcal{L}_{ce}$  with ground truth  $GT$ :

$$\theta_{Seg}^{new} = \theta_{Seg}^{old} + \alpha \nabla_{\theta_{Seg}} \mathcal{L}_{ce}(P_{soft}^t, GT) \quad (3)$$

### 3.4 SAMPLING NET

Given predicted masks  $P_1^t, \dots, P_N^t$ , we first cluster them into  $K$  groups by K-means noa method. Then the clinician selects the potential region  $P_{pref}$  which requires further modification, based on their personal preference. This information is incorporated into prompt embedding  $E_p^t$  through prompt encoder.

We assume that each clinician is independent and identically distributed and their prompt embedding  $E_p^t$  is conditioned on the sampling space  $SP$ . So we can further assume that the sampling space  $SP$  is composed of  $M$  independent and identically distributed Gaussian distributions  $Z_1, \dots, Z_M$ , each with mean  $\mu_m$ , variance  $\sigma_m^2$  and weight  $\pi_m$ , where  $\pi_m > 0$  and  $\sum_{m=1}^M \pi_m = 1$ :

$$P_{pref}^t | Z_i = m \sim N(\mu_m, \sigma_m^2), m = 1, \dots, M \quad (4)$$

Thus, if we represent  $f(P_{pref}^t; \mu_m, \sigma_m^2)$  as the probability density function of a Gaussian distribution with mean  $\mu_m$  and variance  $\sigma_m^2$ , then the posterior distribution of  $Z_i$  given  $P_{pref}^t$  can be written as:

$$P(Z_i = m | P_{pref}^t) = \frac{P(P_{pref}^t | Z_i = m) \cdot P(Z_i = m)}{P_{pref}^t} = \frac{f(P_{pref}^t; \mu_m, \sigma_m^2) \cdot \pi_m}{\sum_{m'}^M f(P_{pref}^t; \mu_{m'}, \sigma_{m'}^2) \cdot \pi_{m'}} \quad (5)$$

Given the image embeddings,  $\mu_m$  and  $\sigma_m^2$  are trained through Mean-Variance Network, which consists of several convolution layers and ReLU activations. In order to update all parameters in the Mean-Variance Network and prompt encoder, we compare the modified prediction  $P_{mod}^t$  with ground truth  $GT$  through the cross-entropy loss function. These parameters are represented as  $\theta_{MVP}^{new}$ , and importantly, all parameters in the segmentation net are frozen:

$$\theta_{MVP}^{new} = \theta_{MVP}^{old} + \alpha \nabla_{\theta_{MVP}} \mathcal{L}_{ce}(P_{mod}^t, GT) \quad (6)$$

Apart from  $\theta_{MVP}^{old}$ , we utilise Weight Network to update  $\pi_m$  through the mean squared error loss function  $\mathcal{L}_{mse}$  with ground truth’s posterior distribution:

$$\theta_W^{new} = \theta_W^{old} + \alpha \nabla_{\theta_W} \mathcal{L}_{mse}(P(Z_i = m | P_{mod}^t), P(Z_i = m | GT)) \quad (7)$$

where  $\mathcal{L}_{mse}$  is the mean-square loss function and  $\theta_W^{new}$  represents all parameters in the weight network. The weight network is composed by simple linear layers and ReLU activations.

## 4 EXPERIMENT

We conducted extensive experiments to verify the effectiveness of our proposed MedUHIP approach across seven multi-clinician annotated medical segmentation tasks, utilising data from various imaging modalities, including colour fundus images, CT, and MRI scans.

## 4.1 DATASET

**REFUGE2** benchmark Fang et al. (2022) is a publicly available fundus image dataset collected for glaucoma analysis, including the optic-cup segmentation task. The fundus images are annotated by seven independent ophthalmologists, each with an average of 8 years of experience. These annotations are then reviewed by a senior specialist with over 10 years of experience in the field. REFUGE2 dataset contains 400 images for training and 400 images for testing.

**LIDC-IDRI** benchmark Armato et al. (2011); Clark et al. (2013) originally consists of 3D lung CT scans with semantic segmentations of possible lung abnormalities. It comprises 1,018 lung CT scans from 1,010 patients, with manual lesion segmentations provided by four radiologists. We use a pre-processed dataset offered by Kohl et al. (2019a), resulting 15,096 2D CT images. After a 80-20 train-test split, our training and testing dataset contains 12,077 and 3,019 images, respectively.

**QUBIQ** benchmark Li et al. (2024) is collected for investigating inter-clinician variability in medical image segmentation tasks. It contains one MRI brain tumour task (three annotations, 28 cases for training, 4 cases for testing); two MRI prostate-related tasks (six annotations, 48 cases for training, 7 cases for testing); one MRI brain-growth task (seven annotations, 34 cases for training, 5 cases for testing); and one CT kidney task (three annotations, 20 cases for training, 4 cases for testing).

## 4.2 EXPERIMENTAL SETUP

Our network was implemented with the PyTorch platform and trained/tested on RTX A4000 with 32GB of memory. During training, we employed the Adam optimizer with an initial learning rate of  $1e^{-4}$  and adjusted the learning rate with StepLR strategy. To ensure fair comparison, we used majority vote to train deterministic methods with multiple annotations. For the SAM-series interaction models, we randomly generated click prompt or bounding box prompt, depending on the original model settings. During the testing stage, a random set of annotations were selected, fused, and binarised. This fused binary segmentation was then used as the ground truth for evaluation. In addition, we consistently utilised vit/b as the backbone when vision transformer was involved in the models.

## 4.3 EXPERIMENTAL RESULT

### 4.3.1 PERFORMANCE ANALYSIS ON DIFFERENT INTERACTION STRATEGY

Table 1: Performance Analysis by Dice Score comparison (%) between different interaction strategies. Columns represent ground truth from combinations of 1 to 7 clinicians’ annotations, comparing different interaction strategies.

Interaction Strategy	1	2	3	4	5	6	7	Ave
Random Select	67.59	71.46	77.29	78.80	82.59	80.41	84.57	79.17
Clinician Disagreement	66.48	71.26	77.76	81.18	84.44	83.21	85.34	80.96
Last Wrong	66.96	73.30	78.84	83.31	86.05	85.72	<b>88.70</b>	82.96
<b>MedUHIP</b>	<b>74.50</b>	<b>79.00</b>	<b>83.52</b>	<b>85.13</b>	<b>87.08</b>	<b>88.10</b>	87.70	<b>85.29</b>

As demonstrated in Section 3.1, segmentation performance varies significantly with different interaction strategies and individual clinician’s preference. We conducted quantitative experiments on the REFUGE2 test set to verify that our MedUHIP approach can generate superior segmentations regardless of the clinician’s interaction strategy. Table 1 presents the segmentation performance measured by Dice Score, evaluated after three human interactions. Each column represents the number of clinicians whose annotations are fused to form the ground truth, ranging from one to seven. The ‘Random Select’, ‘Clinician Disagreement’ and ‘Last Wrong’ strategies follow the definition in Section 3.1.

Table 1 shows that the ‘Random Select’, ‘Clinician Disagreement’ and ‘Last Wrong’ strategies exhibit performance improvements with more fused annotations, averaging 79.17%, 80.96%, and 82.96% respectively. However, our proposed method, MedUHIP, consistently outperforms these approaches. MedUHIP achieves the highest Dice Score in nearly all configurations, with an average Dice Score of 85.29%, highlighting its robustness and effectiveness. Notably, MedUHIP performs comparably or even better than the ‘Last Wrong’ strategy, which emulates the experienced clinicians’ behaviours.

Additionally, MedUHIP reaches its peak performance with a Dice Score of 88.10% when fusing annotations from six clinicians.

#### 4.3.2 PERFORMANCE ANALYSIS WITH STATE-OF-THE-ARTS (SOTA) METHODS

To demonstrate the advantage of the proposed MedUHIP, we compared it with the SOTA methods, classified into deterministic methods (UNet Ronneberger et al. (2015), TransUNet Chen et al. (2021), SwinUNet Cao et al. (2021)), uncertainty-based methods (Ensemble UNet, ProbUNet Kohl et al. (2018), LS-Unet Jensen et al. (2019), MH-Unet Guan et al. (2018), CM-Net Zhang et al. (2020), MRNet Ji et al. (2021)), and interactive methods (SAM Kirillov et al. (2023), MedSAM Ma et al. (2024), MSA Wu et al. (2023)). We also compare with the uncertainty-interactive method SAM-U Deng et al. (2023) with both SAM and MedSAM backbone. For the interactive methods, we include the results after one interaction and three interactions.

Table 2 provides a quantitative performance analysis by comparing Dice Scores across multiple datasets. As shown in Table 2, our proposed MedUHIP after three interactions consistently achieves superior performance compared to other approaches, achieving an average Dice Score of 89.68%. The performance improvement is especially prominent in the LIDC segmentation task, with an increase of  $\sim 20\%$  over the current SOTA methods. These results underscore MedUHIP’s effectiveness and robustness across diverse medical image tasks. In addition, even the performance after one interaction is considerable better than SOTA methods, highlighting its potential to generate superior segmentation with minimal user interaction.

Fig. 4 illustrates the visualisation results produced by our MedUHIP in comparison with other SOTA methods. We present the segmentation after six interactions for interaction models. The ground truth is combined with randomly selected clinicians. It is evident that our model has better capability to adapt to the variability introduced by different clinicians, especially at the boundary regions.

Table 2: Performance Analysis by Dice Score comparison (%) between deterministic models, uncertainty-based models and interactive models.

Methods	REFUGE2	LIDC	BrainTumor	Prostate1	Prostate2	BrainGrowth	Kidney	Ave
UNet Ronneberger et al. (2015)	68.94	62.99	87.30	83.89	77.22	62.02	82.40	74.96
TransUNet Chen et al. (2021)	80.83	64.09	90.14	83.35	68.34	86.58	52.99	75.19
SwinUNet Cao et al. (2021)	78.67	59.45	91.23	82.02	74.19	74.88	69.41	75.69
Ensemble UNet	70.75	63.84	90.56	85.27	79.07	71.69	89.30	78.64
ProbUNet Kohl et al. (2018)	68.93	48.52	89.02	72.13	66.84	75.59	75.73	70.96
LS-Unet Jensen et al. (2019)	73.32	62.05	90.89	87.92	81.59	85.63	72.31	79.10
MH-Unet Guan et al. (2018)	72.33	62.60	86.74	87.03	75.61	83.54	73.44	77.32
MRNet Ji et al. (2021)	80.56	63.29	85.84	87.55	70.82	84.41	61.30	76.25
SAM <sup>3</sup> Kirillov et al. (2023)	82.59	66.68	91.55	92.82	77.04	86.63	85.72	83.29
MedSAM <sup>3</sup> Ma et al. (2024)	82.34	68.42	92.67	89.69	74.70	85.91	78.02	81.68
MSA <sup>3</sup> Wu et al. (2023)	83.03	66.88	88.16	89.06	68.94	80.62	25.29	71.71
SAM-U <sup>3</sup> (SAM backbone) Deng et al. (2023)	82.45	62.24	92.67	81.46	66.56	87.79	89.50	80.38
SAM-U <sup>3</sup> (MedSAM backbone) Deng et al. (2023)	80.66	64.82	93.11	91.89	72.91	87.51	90.74	83.09
<b>MedUHIP<sup>1</sup></b>	<b>83.47</b>	<b>88.07</b>	<b>94.29</b>	<b>93.12</b>	<b>83.34</b>	<b>88.14</b>	<b>94.08</b>	<b>89.22</b>
SAM <sup>3</sup>	82.61	66.71	92.14	92.72	77.54	86.58	90.43	84.10
MedSAM <sup>3</sup>	82.13	68.45	93.26	90.05	73.81	86.09	79.88	81.95
MSA <sup>3</sup>	83.08	66.87	91.25	90.22	71.34	81.87	46.76	75.91
SAM-U <sup>3</sup> (SAM backbone)	82.10	62.84	92.31	81.79	66.74	87.84	89.24	80.40
SAM-U <sup>3</sup> (MedSAM backbone)	80.54	65.44	92.40	90.00	73.17	87.87	91.35	82.96
<b>MedUHIP<sup>3</sup></b>	<b>85.42</b>	<b>88.56</b>	<b>94.31</b>	<b>92.97</b>	<b>84.05</b>	<b>88.18</b>	<b>94.26</b>	<b>89.68</b>

#### 4.3.3 THRESHOLD ANALYSIS ON DIFFERENT INTERACTIVE MODELS

We conducted a threshold analysis to quantify the number of interactions required to reach specific Dice Scores across various interactive models. We ran all models with at most 6 iterations, and assigned the click number to 10 if the image failed to reach the specific Dice Score. Our proposed method, MedUHIP, demonstrated superior efficiency in requiring fewer interactions to achieve high-performance segmentation results compared to other methods.

For the REFUGE2 dataset, MedUHIP only requires 2.72 interactions on average to achieve 80% Dice Score, compared to SAM’s 3.65 and MedSAM’s 3.67 interactions. Similarly, for the LIDC dataset, MedUHIP necessitates just 2.24 interactions, whereas the closest competitor, SAM-U with MedSAM backbone requires 3.86 interactions. Although MedUHIP does not always require the fewest clicks, it remains highly competitive. For example, MedUHIP achieves 2.42 interactions in the Prostate1 task, which is fewer than most models, but slightly more than SAM at 1.57 interactions.

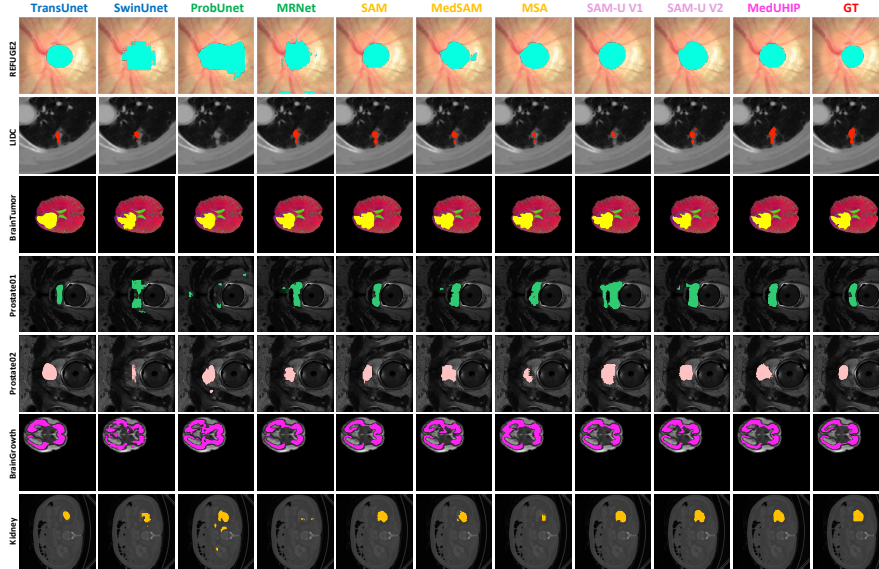


Figure 4: Visualisation results produced by deterministic models, uncertainty-based models, interactive models, our MedUHIP method and the ground truth.

Table 3: Threshold Analysis by Number of Interactions to achieve specific Dice Score between interactive models. If the model fails to achieve the Dice Score in 6 interactions, it is assigned with 10 interactions.

Methods	REFUGE2	LIDC	BrainTumor	Prostate1	Prostate2	BrainGrowth	Kidney
	NoC <sub>80</sub>	NoC <sub>70</sub>	NoC <sub>92</sub>	NoC <sub>90</sub>	NoC <sub>80</sub>	NoC <sub>88</sub>	NoC <sub>90</sub>
SAM	3.65	3.94	2.00	<b>1.57</b>	<b>2.28</b>	4.60	4.25
MedSAM	3.67	3.69	<b>1.00</b>	3.57	3.57	8.20	10.00
MSA	3.54	3.88	5.00	3.00	3.57	10.00	10.00
SAM-U (SAM backbone)	3.98	4.18	4.00	8.71	6.14	4.60	3.75
SAM-U (MedSAM backbone)	4.53	3.86	4.00	3.57	3.57	3.20	3.50
<b>MedUHIP</b>	<b>2.72</b>	<b>2.24</b>	<b>1.00</b>	2.42	<b>2.28</b>	<b>2.80</b>	<b>3.25</b>

#### 4.3.4 SAMPLING SPACE ANALYSIS

We carried out a sampling space analysis to demonstrate that the sampling space captures clinician interaction preference. Fig. 5 represents the hidden space values for different clinicians, sampled from a Gaussian mixture model based on the mean, variance, and weight after six interactions. Each clinician on the horizontal axis has a corresponding boxplot showing the distribution of hidden space values. The similar median values across clinicians suggest that their decisions are roughly similar, while variations indicate personal preferences. It highlights that our model’s hidden space can capture each clinician’s unique interaction preferences.

#### 4.3.5 ABLATION STUDIES

In this section, we performed an ablation study on each component of our proposed MedUHIP model, including random sampling from the hidden space, updating Gaussian distributions’ mean and variance in the hidden space, and updating the weights of Gaussian distributions in the hidden space. The ablation analysis is presented in Table 4, with segmentation performance evaluated by Dice Score for the REFUGE2 and Kidney datasets.

When only sampling from hidden space without calibrating mean, variance, and weight, the Dice Score is 80.29% for REFUGE2 and 90.05% for the Kidney dataset. Training the distributions’ mean and variance in the hidden space boosts segmentation performance to 84.12% and 92.06% for REFUGE2 and Kidney, respectively. Including training distribution weight alone improves the Dice Score to 82.87% for REFUGE2 and 92.29% for Kidney.



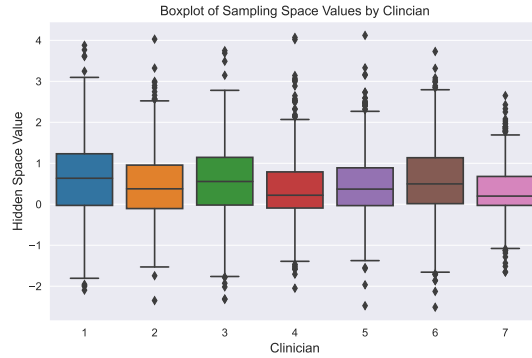


Figure 5: Boxplot of sampling space values based on different clinicians. We draw samples with the mean, variance, weight after six interactions for each clinician.

Finally, combining all three components which results to calibrating distribution mean, variance, and weight before sampling from the hidden space yields the highest performance, with Dice Scores of 85.42% for REFUGE2 and 94.26% for the Kidney dataset. This demonstrates the complementary benefits of each component, highlighting their significance in achieving optimal segmentation performance.

Table 4: Ablation analysis on REFUGE2 and Kidney dataset

Sampling	Mean-Variance	Weight	REFUGE2	Kidney
✓			80.29	90.05
✓	✓		84.12	92.06
✓		✓	82.87	92.29
✓	✓	✓	<b>85.42</b>	<b>94.26</b>

## 5 CONCLUSION

In this work, we introduce MedUHIP, a novel paradigm that integrates an uncertainty-aware model with human-in-the-loop interaction to achieve quantitative segmentations of uncertain medical images under clinician supervision. Our approach feature a Segmentation Net, which generates multiple plausible predictions by sampling to address inherent uncertainties. We then incorporated the clinician interactions to quickly calibrate these predictions toward their preference using the Sampling Net. Extensive empirical experiments have demonstrated the superior performance of MedUHIP across a wide range of medical image segmentation tasks and diverse image modalities, all with fewer interactions. This approach shows great potential for practical implementation in clinical settings.

## REFERENCES

- Advances in K-means Clustering: A Data Mining Thinking | SpringerLink. URL <https://link.springer.com/book/10.1007/978-3-642-29807-3>.
- Samuel G. Armato, Geoffrey McLennan, Luc Bidaut, Michael F. McNitt-Gray, Charles R. Meyer, Anthony P. Reeves, Binsheng Zhao, Denise R. Aberle, Claudia I. Henschke, Eric A. Hoffman, Ella A. Kazerooni, Heber MacMahon, Edwin J. R. van Beek, David Yankelevitz, Alberto M. Biancardi, Peyton H. Bland, Matthew S. Brown, Roger M. Engelmann, Gary E. Laderach, Daniel Max, Richard C. Pais, David P.-Y. Qing, Rachael Y. Roberts, Amanda R. Smith, Adam Starkey, Poonam Batra, Philip Caligiuri, Ali Farooqi, Gregory W. Gladish, C. Matilda Jude, Reginald F. Munden, Iva Petkovska, Leslie E. Quint, Lawrence H. Schwartz, Baskaran Sundaram, Lori E. Dodd, Charles Fenimore, David Gur, Nicholas Petrick, John Freymann, Justin Kirby, Brian Hughes, Alessi Vande Castele, Sangeeta Gupte, Maha Sallam, Michael D. Heath, Michael H. Kuhn, Ekta Dharaiya, Richard Burns, David S. Fryd, Marcos Salganicoff, Vikram Anand, Uri Shreter, Stephen Vastagh, Barbara Y. Croft, and Laurence P. Clarke. The Lung Image Database Consortium (LIDC) and Image Database Resource Initiative (IDRI): A Completed Reference Database of Lung Nodules on CT Scans. *Medical Physics*, 38(2):915–931, February 2011. ISSN 0094-2405. doi: 10.1118/1.3528204. URL <https://www.ncbi.nlm.nih.gov/pmc/articles/PMC3041807/>.
- Christian F. Baumgartner, Kerem C. Tezcan, Krishna Chaitanya, Andreas M. Hötter, Urs J. Muehlemaier, Khoschy Schawkat, Anton S. Becker, Olivio Donati, and Ender Konukoglu. PHiSeg: Capturing Uncertainty in Medical Image Segmentation. In Dinggang Shen, Tianming Liu, Terry M. Peters, Lawrence H. Staib, Caroline Essert, Sean Zhou, Pew-Thian Yap, and Ali Khan (eds.), *Medical Image Computing and Computer Assisted Intervention – MICCAI 2019*, pp. 119–127, Cham, 2019. Springer International Publishing. ISBN 978-3-030-32245-8. doi: 10.1007/978-3-030-32245-8\_14.
- Federico Cabitza, Davide Ciucci, and Raffaele Rasoini. A giant with feet of clay: on the validity of the data that feed machine learning in medicine, May 2018. URL <http://arxiv.org/abs/1706.06838>. arXiv:1706.06838 [cs, stat].
- Hu Cao, Yueyue Wang, Joy Chen, Dongsheng Jiang, Xiaopeng Zhang, Qi Tian, and Manning Wang. Swin-Unet: Unet-like Pure Transformer for Medical Image Segmentation, May 2021. URL <http://arxiv.org/abs/2105.05537>. arXiv:2105.05537 [cs, eess].
- Heang-Ping Chan, Ravi K. Samala, Lubomir M. Hadjiiski, and Chuan Zhou. Deep Learning in Medical Image Analysis. In Gobert Lee and Hiroshi Fujita (eds.), *Deep Learning in Medical Image Analysis : Challenges and Applications*, pp. 3–21. Springer International Publishing, Cham, 2020. ISBN 978-3-030-33128-3. doi: 10.1007/978-3-030-33128-3\_1. URL [https://doi.org/10.1007/978-3-030-33128-3\\_1](https://doi.org/10.1007/978-3-030-33128-3_1).
- Jieneng Chen, Yongyi Lu, Qihang Yu, Xiangde Luo, Ehsan Adeli, Yan Wang, Le Lu, Alan L. Yuille, and Yuyin Zhou. TransUNet: Transformers Make Strong Encoders for Medical Image Segmentation, February 2021. URL <http://arxiv.org/abs/2102.04306>. arXiv:2102.04306 [cs].
- Kenneth Clark, Bruce Vendt, Kirk Smith, John Freymann, Justin Kirby, Paul Koppel, Stephen Moore, Stanley Phillips, David Maffitt, Michael Pringle, Lawrence Tarbox, and Fred Prior. The Cancer Imaging Archive (TCIA): Maintaining and Operating a Public Information Repository. *Journal of Digital Imaging*, 26(6):1045–1057, December 2013. ISSN 0897-1889. doi: 10.1007/s10278-013-9622-7. URL <https://www.ncbi.nlm.nih.gov/pmc/articles/PMC3824915/>.
- Guoyao Deng, Ke Zou, Kai Ren, Meng Wang, Xuedong Yuan, Sancong Ying, and Huazhu Fu. SAM-U: Multi-box prompts triggered uncertainty estimation for reliable SAM in medical image, July 2023. URL <http://arxiv.org/abs/2307.04973>. arXiv:2307.04973 [cs].
- Huihui Fang, Fei Li, Junde Wu, Huazhu Fu, Xu Sun, Jaemin Son, Shuang Yu, Menglu Zhang, Chenglang Yuan, Cheng Bian, Baiying Lei, Benjian Zhao, Xinxing Xu, Shaohua Li, Francisco Fumero, José Sigut, Haidar Almubarak, Yakoub Bazi, Yuanhao Guo, Yating Zhou, Ujjwal Baid, Shubham Innani, Tianjiao Guo, Jie Yang, José Ignacio Orlando, Hrvoje Bogunović, Xiulan Zhang,

- and Yanwu Xu. REFUGE2 Challenge: A Treasure Trove for Multi-Dimension Analysis and Evaluation in Glaucoma Screening, December 2022. URL <http://arxiv.org/abs/2202.08994>. arXiv:2202.08994 [cs, eess].
- Luís P. F. Garcia, André C. P. L. F. de Carvalho, and Ana C. Lorena. Effect of label noise in the complexity of classification problems. *Neurocomputing*, 160:108–119, July 2015. ISSN 0925-2312. doi: 10.1016/j.neucom.2014.10.085. URL <https://www.sciencedirect.com/science/article/pii/S0925231215001241>.
- Melody Y. Guan, Varun Gulshan, Andrew M. Dai, and Geoffrey E. Hinton. Who Said What: Modeling Individual Labelers Improves Classification, January 2018. URL <http://arxiv.org/abs/1703.08774>. arXiv:1703.08774 [cs].
- Kaiming He, Xinlei Chen, Saining Xie, Yanghao Li, Piotr Dollár, and Ross Girshick. Masked Autoencoders Are Scalable Vision Learners, December 2021. URL <http://arxiv.org/abs/2111.06377>. arXiv:2111.06377 [cs].
- Mohammad Hesam Hesamian, Wenjing Jia, Xiangjian He, and Paul Kennedy. Deep Learning Techniques for Medical Image Segmentation: Achievements and Challenges. *Journal of Digital Imaging*, 32(4):582–596, August 2019. ISSN 1618-727X. doi: 10.1007/s10278-019-00227-x. URL <https://doi.org/10.1007/s10278-019-00227-x>.
- Ling Huang, Su Ruan, Yucheng Xing, and Mengling Feng. A review of uncertainty quantification in medical image analysis: Probabilistic and non-probabilistic methods. *Medical Image Analysis*, 97:103223, October 2024. ISSN 1361-8415. doi: 10.1016/j.media.2024.103223. URL <https://www.sciencedirect.com/science/article/pii/S1361841524001488>.
- Martin Holm Jensen, Dan Richter Jørgensen, Raluca Jalaboi, Mads Eiler Hansen, and Martin Aastrup Olsen. Improving Uncertainty Estimation in Convolutional Neural Networks Using Inter-rater Agreement. In Dinggang Shen, Tianming Liu, Terry M. Peters, Lawrence H. Staib, Caroline Essert, Sean Zhou, Pew-Thian Yap, and Ali Khan (eds.), *Medical Image Computing and Computer Assisted Intervention – MICCAI 2019*, pp. 540–548, Cham, 2019. Springer International Publishing. ISBN 978-3-030-32251-9. doi: 10.1007/978-3-030-32251-9\_59.
- Wei Ji, Shuang Yu, Junde Wu, Kai Ma, Cheng Bian, Qi Bi, Jingjing Li, Hanruo Liu, Li Cheng, and Yefeng Zheng. Learning Calibrated Medical Image Segmentation via Multi-rater Agreement Modeling. In *2021 IEEE/CVF Conference on Computer Vision and Pattern Recognition (CVPR)*, pp. 12336–12346, June 2021. doi: 10.1109/CVPR46437.2021.01216. URL <https://ieeexplore.ieee.org/document/9578194>. ISSN: 2575-7075.
- Alexander Kirillov, Eric Mintun, Nikhila Ravi, Hanzi Mao, Chloe Rolland, Laura Gustafson, Tete Xiao, Spencer Whitehead, Alexander C. Berg, Wan-Yen Lo, Piotr Dollár, and Ross Girshick. Segment Anything, April 2023. URL <http://arxiv.org/abs/2304.02643>. arXiv:2304.02643 [cs].
- Armen Der Kiureghian and Ove Ditlevsen. Aleatory or epistemic? Does it matter? *Structural Safety*, 31(2):105–112, March 2009. ISSN 0167-4730. doi: 10.1016/j.strusafe.2008.06.020. URL <https://www.sciencedirect.com/science/article/pii/S0167473008000556>.
- Simon A. A. Kohl, Bernardino Romera-Paredes, Clemens Meyer, Jeffrey De Fauw, Joseph R. Ledsam, Klaus H. Maier-Hein, S. M. Ali Eslami, Danilo Jimenez Rezende, and Olaf Ronneberger. A Probabilistic U-Net for Segmentation of Ambiguous Images, June 2018. URL <https://arxiv.org/abs/1806.05034v4>.
- Simon A. A. Kohl, Bernardino Romera-Paredes, Klaus H. Maier-Hein, Danilo Jimenez Rezende, S. M. Ali Eslami, Pushmeet Kohli, Andrew Zisserman, and Olaf Ronneberger. A Hierarchical Probabilistic U-Net for Modeling Multi-Scale Ambiguities, May 2019a. URL <http://arxiv.org/abs/1905.13077>. arXiv:1905.13077 [cs].
- Simon A. A. Kohl, Bernardino Romera-Paredes, Clemens Meyer, Jeffrey De Fauw, Joseph R. Ledsam, Klaus H. Maier-Hein, S. M. Ali Eslami, Danilo Jimenez Rezende, and Olaf Ronneberger. A Probabilistic U-Net for Segmentation of Ambiguous Images, January 2019b. URL <http://arxiv.org/abs/1806.05034>. arXiv:1806.05034 [cs, stat].

- Balaji Lakshminarayanan, Alexander Pritzel, and Charles Blundell. Simple and Scalable Predictive Uncertainty Estimation using Deep Ensembles, November 2017. URL <http://arxiv.org/abs/1612.01474>. arXiv:1612.01474 [cs, stat].
- Hongwei Bran Li, Fernando Navarro, Ivan Ezhov, Amirhossein Bayat, Dhritiman Das, Florian Kofler, Suprosanna Shit, Diana Waldmannstetter, Johannes C. Paetzold, Xiaobin Hu, Benedikt Wiestler, Lucas Zimmer, Tamaz Amiranashvili, Chinmay Prabhakar, Christoph Berger, Jonas Weidner, Michelle Alonso-Basant, Arif Rashid, Ujjwal Baid, Wesam Adel, Deniz Ali, Bhakti Baheti, Yingbin Bai, Ishaan Bhatt, Sabri Can Cetindag, Wenting Chen, Li Cheng, Prasad Dutand, Lara Dular, Mustafa A. Elattar, Ming Feng, Shengbo Gao, Henkjan Huisman, Weifeng Hu, Shubham Innani, Wei Jiat, Davood Karimi, Hugo J. Kuijff, Jin Tae Kwak, Hoang Long Le, Xiang Lia, Huiyan Lin, Tongliang Liu, Jun Ma, Kai Ma, Ting Ma, Ilkay Oksuz, Robbie Holland, Arlindo L. Oliveira, Jimut Bahan Pal, Xuan Pei, Maoying Qiao, Anindo Saha, Raghavendra Selvan, Linlin Shen, Joao Lourenco Silva, Ziga Spiclin, Sanjay Talbar, Dadong Wang, Wei Wang, Xiong Wang, Yin Wang, Ruiling Xia, Kele Xu, Yanwu Yan, Mert Yergin, Shuang Yu, Lingxi Zeng, YingLin Zhang, Jiachen Zhao, Yefeng Zheng, Martin Zukovec, Richard Do, Anton Becker, Amber Simpson, Ender Konukoglu, Andras Jakab, Spyridon Bakas, Leo Joskowicz, and Bjoern Menze. QUBIQ: Uncertainty Quantification for Biomedical Image Segmentation Challenge, June 2024. URL <http://arxiv.org/abs/2405.18435>. arXiv:2405.18435 [cs, eess].
- Geert Litjens, Thijs Kooi, Babak Ehteshami Bejnordi, Arnaud Arindra Adiyoso Setio, Francesco Ciompi, Mohsen Ghafoorian, Jeroen A. W. M. van der Laak, Bram van Ginneken, and Clara I. Sánchez. A Survey on Deep Learning in Medical Image Analysis. *Medical Image Analysis*, 42:60–88, December 2017. ISSN 13618415. doi: 10.1016/j.media.2017.07.005. URL <http://arxiv.org/abs/1702.05747>. arXiv:1702.05747 [cs].
- Xiangbin Liu, Liping Song, Shuai Liu, and Yudong Zhang. A Review of Deep-Learning-Based Medical Image Segmentation Methods. *Sustainability*, 13(3):1224, January 2021. ISSN 2071-1050. doi: 10.3390/su13031224. URL <https://www.mdpi.com/2071-1050/13/3/1224>. Number: 3 Publisher: Multidisciplinary Digital Publishing Institute.
- Xiangde Luo, Guotai Wang, Tao Song, Jingyang Zhang, Michael Aertsen, Jan Deprest, Sebastien Ourselin, Tom Vercauteren, and Shaoting Zhang. MIDeepSeg: Minimally Interactive Segmentation of Unseen Objects from Medical Images Using Deep Learning. *Medical Image Analysis*, 72:102102, August 2021. ISSN 13618415. doi: 10.1016/j.media.2021.102102. URL <http://arxiv.org/abs/2104.12166>. arXiv:2104.12166 [cs].
- Jun Ma, Yuting He, Feifei Li, Lin Han, Chenyu You, and Bo Wang. Segment Anything in Medical Images. *Nature Communications*, 15(1):654, January 2024. ISSN 2041-1723. doi: 10.1038/s41467-024-44824-z. URL <http://arxiv.org/abs/2304.12306>. arXiv:2304.12306 [cs, eess].
- Zdravko Marinov, Paul F. Jäger, Jan Egger, Jens Kleesiek, and Rainer Stiefelhagen. Deep Interactive Segmentation of Medical Images: A Systematic Review and Taxonomy, January 2024. URL <http://arxiv.org/abs/2311.13964>. arXiv:2311.13964 [cs, eess].
- Xueyan Mei, Hao-Chih Lee, Kai-yue Diao, Mingqian Huang, Bin Lin, Chenyu Liu, Zongyu Xie, Yixuan Ma, Philip M. Robson, Michael Chung, Adam Bernheim, Venkatesh Mani, Claudia Calcagno, Kunwei Li, Shaolin Li, Hong Shan, Jian Lv, Tongtong Zhao, Junli Xia, Qihua Long, Sharon Steinberger, Adam Jacobi, Timothy Deyer, Marta Luksza, Fang Liu, Brent P. Little, Zahi A. Fayad, and Yang Yang. Artificial intelligence-enabled rapid diagnosis of patients with COVID-19. *Nature Medicine*, 26(8):1224–1228, August 2020. ISSN 1546-170X. doi: 10.1038/s41591-020-0931-3. URL <https://www.nature.com/articles/s41591-020-0931-3>. Publisher: Nature Publishing Group.
- Olaf Ronneberger, Philipp Fischer, and Thomas Brox. U-Net: Convolutional Networks for Biomedical Image Segmentation, May 2015. URL <http://arxiv.org/abs/1505.04597>. arXiv:1505.04597 [cs].
- Christian Rupprecht, Iro Laina, Robert DiPietro, Maximilian Baust, Federico Tombari, Nassir Navab, and Gregory D. Hager. Learning in an Uncertain World: Representing Ambiguity

- Through Multiple Hypotheses, August 2017. URL <http://arxiv.org/abs/1612.00197>. arXiv:1612.00197 [cs].
- Tomas Sakinis, Fausto Milletari, Holger Roth, Panagiotis Korfiatis, Petro Kostandy, Kenneth Philbrick, Zeynettin Akkus, Ziyue Xu, Daguang Xu, and Bradley J. Erickson. Interactive segmentation of medical images through fully convolutional neural networks, March 2019. URL <http://arxiv.org/abs/1903.08205>. arXiv:1903.08205 [cs].
- Aneeta Sylolypavan, Derek Sleeman, Honghan Wu, and Malcolm Sim. The impact of inconsistent human annotations on AI driven clinical decision making. *npj Digital Medicine*, 6(1):1–13, February 2023. ISSN 2398-6352. doi: 10.1038/s41746-023-00773-3. URL <https://www.nature.com/articles/s41746-023-00773-3>. Publisher: Nature Publishing Group.
- Nima Tajbakhsh, Jae Y. Shin, Suryakanth R. Gurudu, R. Todd Hurst, Christopher B. Kendall, Michael B. Gotway, and Jianming Liang. Convolutional Neural Networks for Medical Image Analysis: Full Training or Fine Tuning? *IEEE Transactions on Medical Imaging*, 35(5):1299–1312, May 2016. ISSN 0278-0062, 1558-254X. doi: 10.1109/TMI.2016.2535302. URL <http://arxiv.org/abs/1706.00712>. arXiv:1706.00712 [cs].
- Matthew Tancik, Pratul P. Srinivasan, Ben Mildenhall, Sara Fridovich-Keil, Nithin Raghavan, Utkarsh Singhal, Ravi Ramamoorthi, Jonathan T. Barron, and Ren Ng. Fourier Features Let Networks Learn High Frequency Functions in Low Dimensional Domains, June 2020. URL <http://arxiv.org/abs/2006.10739>. arXiv:2006.10739 [cs].
- Guotai Wang, Wenqi Li, Maria A. Zuluaga, Rosalind Pratt, Premal A. Patel, Michael Aertsen, Tom Doel, Anna L. David, Jan Deprest, Sebastien Ourselin, and Tom Vercauteren. Interactive Medical Image Segmentation using Deep Learning with Image-specific Fine-tuning. *IEEE Transactions on Medical Imaging*, 37(7):1562–1573, July 2018. ISSN 0278-0062, 1558-254X. doi: 10.1109/TMI.2018.2791721. URL <http://arxiv.org/abs/1710.04043>. arXiv:1710.04043 [cs].
- Guotai Wang, Maria A. Zuluaga, Wenqi Li, Rosalind Pratt, Premal A. Patel, Michael Aertsen, Tom Doel, Anna L. David, Jan Deprest, Sebastien Ourselin, and Tom Vercauteren. DeepIGeoS: A Deep Interactive Geodesic Framework for Medical Image Segmentation. *IEEE Transactions on Pattern Analysis and Machine Intelligence*, 41(7):1559–1572, July 2019a. ISSN 0162-8828, 2160-9292, 1939-3539. doi: 10.1109/TPAMI.2018.2840695. URL <http://arxiv.org/abs/1707.00652>. arXiv:1707.00652 [cs].
- Jian Wang, Hengde Zhu, Shui-Hua Wang, and Yu-Dong Zhang. A Review of Deep Learning on Medical Image Analysis. *Mobile Networks and Applications*, 26(1):351–380, February 2021. ISSN 1572-8153. doi: 10.1007/s11036-020-01672-7. URL <https://doi.org/10.1007/s11036-020-01672-7>.
- Li Wang, Dong Nie, Guannan Li, Élodie Puybareau, Jose Dolz, Qian Zhang, Fan Wang, Jing Xia, Zhengwang Wu, Jiawei Chen, Kim-Han Thung, Toan Duc Bui, Jitae Shin, Guodong Zeng, Guoyan Zheng, Vladimir S. Fonov, Andrew Doyle, Yongchao Xu, Pim Moeskops, Josien P.W. Pluim, Christian Desrosiers, Ismail Ben Ayed, Gerard Sanroma, Oualid M. Benkarim, Adrià Casamitjana, Verónica Vilaplana, Weili Lin, Gang Li, and Dinggang Shen. Benchmark on Automatic 6-month-old Infant Brain Segmentation Algorithms: The iSeg-2017 Challenge. *IEEE transactions on medical imaging*, pp. 10.1109/TMI.2019.2901712, February 2019b. ISSN 0278-0062. doi: 10.1109/TMI.2019.2901712. URL <https://www.ncbi.nlm.nih.gov/pmc/articles/PMC6754324/>.
- Junde Wu, Wei Ji, Yuanpei Liu, Huazhu Fu, Min Xu, Yanwu Xu, and Yueming Jin. Medical SAM Adapter: Adapting Segment Anything Model for Medical Image Segmentation, December 2023. URL <http://arxiv.org/abs/2304.12620>. arXiv:2304.12620 [cs].
- Le Zhang, Ryutaro Tanno, Mou-Cheng Xu, Chen Jin, Joseph Jacob, Olga Ciccarelli, Frederik Barkhof, and Daniel C. Alexander. Disentangling Human Error from the Ground Truth in Segmentation of Medical Images, October 2020. URL <http://arxiv.org/abs/2007.15963>. arXiv:2007.15963 [cs].

Wentao Zhu, Yufang Huang, Liang Zeng, Xuming Chen, Yong Liu, Zhen Qian, Nan Du, Wei Fan, and Xiaohui Xie. AnatomyNet: Deep learning for fast and fully automated whole-volume segmentation of head and neck anatomy. *Medical Physics*, 46(2):576–589, 2019. ISSN 2473-4209. doi: 10.1002/mp.13300. URL <https://onlinelibrary.wiley.com/doi/abs/10.1002/mp.13300>. \_eprint: <https://onlinelibrary.wiley.com/doi/pdf/10.1002/mp.13300>.

Ke Zou, Zhihao Chen, Xuedong Yuan, Xiaojing Shen, Meng Wang, and Huazhu Fu. A Review of Uncertainty Estimation and its Application in Medical Imaging, May 2023. URL <http://arxiv.org/abs/2302.08119>. arXiv:2302.08119 [cs, eess].